Chemical Characterization Using Different Analytical Techniques to Understand Processes: The Case of the Paraffinic Base Oil Production Line

Rémi Moulian, Johann Le Maître, Hélène Leroy, Ryan Rodgers, Brice Bouyssière, Carlos Afonso, Pierre Giusti, Caroline Barrère-Mangote

processes

MDPI

Article

Chemical Characterization Using Different Analytical Techniques to Understand Processes: The Case of the Paraffinic Base Oil Production Line

Rémi Moulian [1,2,3], Johann Le Maître [2,3,4], Hélène Leroy [2], Ryan Rodgers [1,2,5,6,7], Brice Bouyssiere [1,2,*], Carlos Afonso [2,4], Pierre Giusti [2,3] and Caroline Barrère-Mangote [2,3,*]

1 E2S UPPA, CNRS, IPREM, Institut des Sciences Analytiques et de Physico-chimie pour l'Environnement et les Materiaux, Universite de Pau et des Pays de l'Adour, UMR5254, Hélioparc, 64053 Pau, France; remi.moulian@gmail.com (R.M.); rrodgers@fsu.edu (R.R.)
2 International Joint Laboratory—iC2MC: Complex Matrices Molecular Characterization, TRTG, BP 27, 76700 Harfleur, France; johann.lemaitre@yahoo.com (J.L.M.); helene.leroy@total.com (H.L.); carlos.afonso@univ-rouen.fr (C.A.); pierre.giusti@total.com (P.G.)
3 TOTAL Refining and Chemicals, Normandy Platform, 76700 Harfleur, France
4 COBRA, UMR 6014 et FR 3038, INSA de Rouen, CNRS, IRCOF, Normandie Université, Université de Rouen, 76130 Mont Saint Aignan CEDEX, France
5 National High Magnetic Field Laboratory, Florida State University, 1800 East Paul Dirac Drive, Tallahassee, FL 32310, USA
6 Department of Chemistry and Biochemistry, 95 Chieftain Way, Florida State University, Tallahassee, FL 32306, USA
7 Future Fuels Institute, 1800 Paul Dirac Drive, Tallahassee, FL 32310–4005, USA
* Correspondence: brice.bouyssiere@univ-pau.fr (B.B.); caroline.mangote@total.com (C.B.-M.); Tel.: +33-0-559-407-752 (B.B.); +33-0-235 551-102 (C.B.-M.)

Received: 11 October 2020; Accepted: 12 November 2020; Published: 18 November 2020

Abstract: Mineral base oils are used to produce commercial lubricants and are obtained from refining vacuum residue. Lubricants are used to reduce friction in industry devices, so their viscosity is a key characteristic that needs to be optimized throughout the process. The purpose of this study is to show how global chemical characterization of samples from the base oil production chain can facilitate a better understanding of the molecular impacts of processing and their effect on macroscopic properties like viscosity. Eight different samples were characterized by different analytical techniques, including liquid chromatography and mass spectrometry techniques, to understand their chemical evolution through the different process units at the molecular level. Furthermore, a statistical treatment allowed for the identification of parameters that influence viscosity, mainly sulfur and polyaromatics content. This study demonstrates the importance and effectiveness of cross-checking results from different complementary analytical techniques to acquire valuable data on lubricating oil base samples.

Keywords: lubricant base oil; GPC ICP HRMS; APPI FT ICR MS; HPLC3; aromatics; viscosity

1. Introduction

High viscosity grade lubricants are used as marine lubricants to reduce friction in slow-speed engine cylinder oils. As for other lubricants, they are composed of a base oil and additives packages that aimed to neutralize acidic combustion by-products, providing detergency or cleaning effect, preventing deposit formation by keeping deposit precursors soluble in the oil (dispersant) and reducing friction and wear. For these high viscosity grade lubricants, base oil or solvent-extracted bright stock, is most commonly obtained by solvent refining. The viscosity (between 30.0 and 35.0 mm^2/s (cSt) at 100 °C), the viscosity index, and pour point are key characteristics of these samples that need to be optimized

throughout the refining process. The viscosity index (VI) is the rate of change in viscosity with changes in temperature while pour point is the temperature below which the liquid loses its flow characteristics.

The solvent extracted bright stock (BSS) is produced from crude oil vacuum residue (VR) by precipitating asphaltenes with liquid propane; this step allows for the optimization of the oil viscosity [1]. The Common "contaminants" in the deasphalted oil (DAO) are aromatic and naphthenic hydrocarbon species, which must be removed to increase the viscosity index [2]. The extraction process consists of treating the DAO with a solvent (furfural (FF) [3] or n-methyl-pyrrolidone), which yields an extract rich in aromatic molecules and a raffinate fraction rich in paraffin [2]. Finally, during the dewaxing process, the raffinate is treated with methyl ethyl ketone (MEK) and toluene to selectively precipitate the n-paraffin from the oils and to optimize the pour point. These different refining steps are aimed at optimizing the viscosity properties (viscosity, viscosity index, pour point, etc.) of the lubricant [2]. Also, commercial specifications, like the aniline point for the lube extract and viscosity for the wax, have to be reached for the co-products of the solvent refining. For this purpose, the different process units are tuned to optimize the different properties of the products.

To obtain a better understanding of the refining processes, it is important to have good chemical characterization of the samples at each step. For base oils, some studies have been published. For example, Mehrkesh et al. [2] found a correlation between the aromatics content of six raffinate samples and their viscosity, regardless of temperature. Varotsis and Pasadakis [4] developed a method to determine the percentage of monoaromatics, diaromatics, and triaromatics using a gel permeation chromatography (GPC)-UV-RI system. They used the differences in the absorption wavelengths of each compound to calculate the amount of each compound in the sample. In this work, Pasadakis showed that aromatics can be determined by a simple technique, such as GPC-UV, in these types of samples. Alawani et al. [5] suggested that the aromaticity of compounds found in crude oil samples increases with increasing elution time in GPC when using toluene as the mobile phase.

Mass spectrometry techniques are also useful for the characterization of base oil samples. Wang and Zhang [6] used GC-MS and found a correlation between the isoparaffins index and viscosity after the dewaxing process. Manheim et al. and Liang et al. [7,8] used a gas chromatography 2D (GC × GC)/EI TOF mass spectrometer to identify and quantitate linear alkanes. Linear alkanes negatively affect the performance of lubricant base oils. Desprez et al. [9] used GPC with inductively coupled plasma mass spectrometry (GPC-ICP HR MS) to correlate the viscosity and sulfur aggregation behavior in crude oil, atmospheric residue (AR), vacuum gas oil (VGO) and VR samples. Panda et al. [10] fractionated crude oil by preparative GPC and analyzed it using atmospheric pressure photo ionization (APPI) and Fourier transformation ion cyclotron resonance mass spectrometry (FT-ICR MS). They found that the more the retention time increased, the more the aromaticity of the samples increased. Putman et al. [11] obtained similar results; they observed that more aliphatic compounds have a greater tendency to aggregate, leading to a reduced retention time. Duan et al. [12] and Nyadong et al. [13] each used laser-induced acoustic desorption with different chemical ionization (LIAD-CI) methods, atmospheric pressure chemical ionization (APCI) [13] and with the aqua chloromanganese II cation [12], to determine the molecular mass of the compounds present as well as the percentage of saturate, monoaromatics, and diaromatics in lubricant oils. Hourani et al. [14] used high performance liquid chromatography (HPLC), gas chromatography 2D (GC × GC) and FT-ICR MS to identify mono-, di-, and triaromatic compounds in lubricant base oil. For FT-ICR MS, they used two different ionization techniques, APPI and APCI, which allowed them to determine the molecular structure of the base oils. Furthermore, they found that APCI was more effective for studying saturated compounds. These works showed the importance of mass spectrometry for acquiring molecular information about paraffinic and polyaromatic species, which are key parameters in lubricant base oil samples.

According to the literature [2,4,5], the content of aromatics and sulfur in base oils had an impact on their viscosity as well as on the aniline point for lube extract. In this work, samples from all phases of the lubricant oil production line, from vacuum residue to bright stock solvent and wax, were characterized and compared. Three main techniques were used to provide different information.

First, HPLC with an evaporative light scattering detector (ELSD) was used to obtain information about the quantity of saturate, mono-, and polyaromatic compounds. This method, referred to as HPLC3, was previously described by Putman et al. [15]. HPLC3 provides information on the percentage of saturates and aromatics. Then, GPC with inductively coupled plasma mass spectrometry (ICP HR MS) was used to analyze the sulfur and vanadium containing compounds in each sample. This technique can be used to quantify the sulfur and vanadium present in the sample, but more importantly, it provides information on the aggregation state of vanadium- and sulfur-containing molecules. Then, APPI [14–17]/APCI [18–22]-FT-ICR MS [23–26] was used to obtain molecular data of the different samples. In particular, information was obtained on the degree of aromaticity of sulfur [27,28] and hydrocarbon molecules. In the present study, 8 samples were analyzed, and all the data collected were correlated with the viscosity [29] of each sample. Statistical treatment using partial least square (PLS) regression was performed to determine which parameters affect viscosity [30].

2. Materials and Methods

2.1. Samples, Materials, and Reagents

The three units of the production line, solvent de-asphalter (SDA), furfural, and dewaxing, were studied separately to examine potential "tank" effects as described in Figure 1. Eight industrial samples were available.

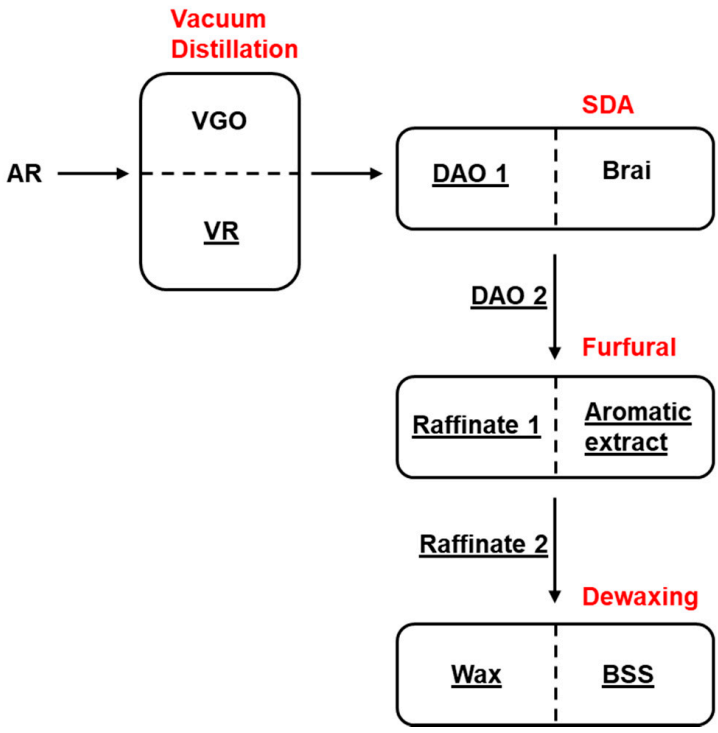

Figure 1. Lubricant oil production scheme.

Vacuum residue (VR) and the corresponding desulphated oil (DAO 1) were obtained with propane in the SDA unit. The other effluent of the SDA unit, which contains the asphaltene fraction and is referred to as brai, was not available for study. Thus, a similar DAO feed of furfural (FF), referred to as DAO 2, with the corresponding effluents raffinate 1 and aromatic extract, was studied. Finally, a similar raffinate sample, the feed of the dewaxing unit, referred to as raffinate 2 with corresponding wax and BSS, was available. This sample was obtained with methyl ether ketone and toluene as the dewaxing solvent.

2.2. Analytical Techniques

2.2.1. HPLC3

As in previous works, the HPLC3 system came from commercially available components [15]. A Waters HPLC system composed of an Alliance e2695 Separation Module, of a WAT 005.319 2 µM as precolumn inline filter, of a 2998 photodiode array and of a 2424 evaporative light scattering detector (ELSD) operated with EMPOWER3 software (Waters, Milford, MA, USA) were used. Two columns were used, the first column was a Chromegabond Dinitroanilinopropyl (DNAP, 4.6 × 250 mm, 5 µM) with a 3.2 × 10 mm Chromegabond DNAP as guard cartridge (ES Industries, West Berlin, NJ, USA). The other column was a Spherisorb strong cation exchange (SCX, 4.6 × 250 mm, 5 µM) (Waters, Milford, MA). To ensure metal saturation of the SCX column to yield the desired Ag-SCX column, a solution of 30 mg/mL silver nitrate in acetonitrile was sent through the column before analysis. A postcolumn dilution using cyclohexane was utilized to facilitate a uniform ELSD response throughout the gradient. The analyses were made with an injection of 40 µL of sample at a concentration of 40 mg/mL during 140 min for each run. The temperature of the columns was not controlled. Only the sample wax was not analyzed with this technique because of its insolubility with the solvent. For data treatment, an external calibration curve was used to determine the percentage in mass for each peak. All the samples were analyzed in triplicate and standard deviations were below 2%.

2.2.2. GPC ICP HR MS

The carrier solution was delivered by a Dionex High-Performance Liquid Chromatography (HPLC) system with an UltiMate 3000 microflow pump and an UltiMate 3000 autosampler. THF and Multisolvent® GPC-grade ACS stabilized with 250 ppm of BHT (Scharlau) were used as solvents for the dilution of samples and as mobile phases. Chromatographic separation was performed by three GPC columns (from 1000 to 600,000 Dalton) connected in series. A Styragel guard column (4.6 mm inner diameter, 30 mm length, 10,000 Da exclusion limit) was used as the guard column. Twenty microliters of solution were injected and eluted at 1 mL min^{-1} of THF for 90 min. A postcolumn splitter was used to send 40 µL min^{-1} in the ICP HR MS, sending the other part to the waste. Samples were analyzed a maximum of a few hours after preparation.

As in our previous works [9,11,31], the introduction system of the mass spectrometer used in this work is a modified DS-5 microflow total consumption nebulizer (CETAC, Omaha, NE, USA) mounted with a laboratory-made glass spray chamber already used during prior study [31–33]. The temperature was maintained at 60 °C using a temperature-controlled bath with water (Neslab RTE-111, Thermo Fisher Scientific, Waltham, MA, USA). An argon gas flow was used at 16 L min^{-1} as plasma, an argon auxiliary gas was used at 0.9 L min^{-1} and an argon nebulizer gaz was used at 0.6 L min^{-1}. An O_2 gas flow was added to avoid carbon deposition at 0.08 L min^{-1}. The mass spectrometer was equipped with a quartz injector (inner diameter 1.0 mm), a Pt sampler (orifice diameter 1.1 mm) and skimmer (orifice diameter 0.8 mm) cones. With a double-focusing sector field inductively coupled plasma mass spectrometer (Element XR, Thermo Fisher Scientific, Bremen, Germany), enough resolution was obtained to avoid the spectrally interfered isotopes of ^{32}S, ^{51}V.

2.2.3. APPI/APCI FTICR-MS

Toluene was used to dissolve the samples; the samples were then diluted in methanol/toluene (50/50 v/v) until a concentration of 0.5 mg mL^{-1} was reached, for APPI analysis. The BSS and wax samples were dissolved and diluted in heptane at a concentration of 0.5 mg mL^{-1} for APCI analysis.

A hybrid quadrupole FT-ICR instrument (SolariXR, Bruker Daltonics, Bremen, Germany) equipped with a 12 T superconducting magnet was operated using APPI (10/10.6 eV, Kr-lamp) and the APCI source [19]. Mass spectra were acquired with a mass range of m/z 147–1300 for 128 scans from broadband experiments. The signal was digitalized with 8 M points, giving a transient length of 3.4 s. The accumulation time was set to 0.025 s at a flow rate of 600 µL h^{-1}. The experimental conditions

were: desolvation gas flow of 3 L min^{-1}, vaporizer temperature of 300 °C, source temperature of 220 °C, capillary voltage of −900 V in APPI and −4000 V in APCI, corona needle of 9000 nA in APCI, nebulizer pressure of 2.5 bar, octopole energy of 350 Vpp, quadrupole lower cut-off *m*/*z* 200, quadrupole collision energy 1 of 200 Vpp, and TOF duration of 0.8 ms. A blank was recorded during 8 min prior to the introduction of each sample.

Mass spectrometers were externally calibrated using a sodium trifluoroacetate solution before sample analyses. Data Analysis (version 4.4) was used for instrument control and data acquisition. PetroOrg (version 9.4.1), CERES (self-developed Matlab-based interface) and OriginPro (version 2016) were used to process the data [34].The molecular formulas were determined from the accurate mass measurements (typically <0.2 ppm). The number of double bond equivalents (DBEs) were calculated from Equation (1) (*c*: carbon number; *h*: hydrogen number; *n*: nitrogen number) for a molecule of the crude formula $C_cH_hN_nO_oS_s$ [35]. Given a resolving power of 0.9×10^6 at *m*/*z* 400, it is possible to separate class C_xH_y ions from class S_1 (mass split: 3.4 mDa) compounds.

$$DBE = c - \frac{h}{2} + \frac{n}{2} + 1 \quad (1)$$

2.2.4. Statistical Treatment Using Partial Least Square (PLS) Regression

All the data acquired using the three different techniques, as well as the easily acquired refinery data given in Table 1, were used for the statistical treatment. The crystallizable fraction (CF) parameter represents the percentage of normal paraffin in wax obtained by differential scanning calorimetry (DSC). DSC measured the temperature of the transition between solid and liquid of one sample. This temperature made it possible to determine the quantity crystallizable paraffin in the sample. Conradson carbon residue (CCR) then represents the quantity of matter remaining after evaporation and pyrolysis of the sample.

Table 1. Measurable data of different samples.

		Sulfur Content (%w)	Vanadium Content (ppm)	Carbon Content (%w)	Hydrogen Content (%w)	Viscosity at 100 °C (cSt)	Crystallizable Fraction (FC, %w)	Carbon Conradson (CCR, %w)
SDA	**VR**	2.95	150	85.6	10.9	353.8	5.7	15.36
	DAO 1	1.67	1.6	85.9	12.5	33.83	12.7	1.65
FF	**DAO 2**	1.70	2.2	85.3	12.5	34.52	12.2	2.01
	Raffinate 1	0.83	<0.1	85.9	13.4	26.72	19.6	0
	Aromatic Extract	2.80	4.8	84.5	11.1	61.39	3.2	0
Dewaxing	**Raffinate 2**	0.77	<0.1	85.7	13.5	29.79	21.4	0.34
	BSS	0.94	<0.1	86.2	13.3	31.87	6.3	0.53
	Wax	0.38	<0.1	85.2	14.2	17.31	72.7	0

Statistical treatment by partial least square (PLS) analysis was used to determine which parameters affected viscosity: % carbon, % hydrogen, % sulfur, % saturate, % one ring, % 2−5 rings, crystallizable fraction (FC), CCR, retention time at maximum intensity for ^{32}S (GPC-ICP HR MS), ratio x_2/x_1 (GPC-ICP HR MS), and all the parameters given by FT-ICR MS for the CH and S_1 maps: nC/DBE minimum, nC/DBE maximum, and plot size nC/DBE.

3. Results

This section is divided by subheadings. It provides a concise and precise description of the experimental results, their interpretation, as well as the experimental conclusions that can be drawn.

3.1. HPLC3 Results

HPLC3 makes it possible to fractionate and quantify the saturate (Sat), 1−ring aromatic, 2−ring aromatic, 3−ring aromatic, 4−ring aromatic, and 5+ aromatic and polar compounds present in the samples. All the samples were analyzed, with the exception of wax, for solubility reasons. The results are shown for each process unit in Figure 2.

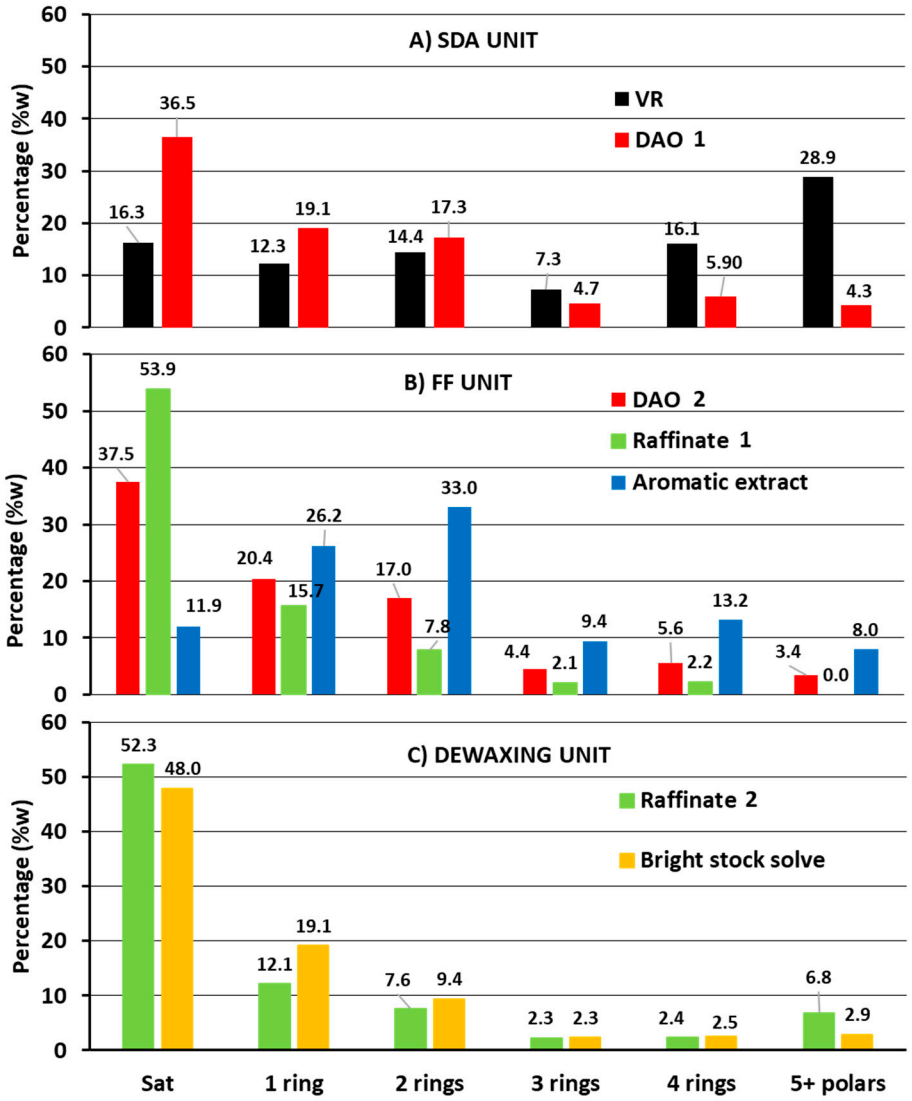

Figure 2. Percentage (%w) of saturate and aromatics by high performance liquid chromatography (HPLC) with an evaporative light scattering detector (ELSD) (HPLC3) for solvent de-asphalter (SDA) (**A**), furfural (FF) (**B**) and (**C**) DEWAXING units.

Figure 2A presents the percentage of different fractions for the SDA UNIT samples, VR and DAO 1. As expected, in Figure 2A, when comparing DAO 1 with VR, note the significant decreases of polyaromatics and polars (5+ polar, 4 rings, and 3 rings). This result means that the highly aromatic and polar components, which are not soluble in propane, enter the brai fraction. Moreover, note that, for DAO 1, the saturated and weakly aromatic compounds (1 ring and 2 rings) increased in proportion.

Figure 2B presents the percentage of different fractions of the FF unit samples. As expected, in Figure 2B, the aromatic extract contains a higher content of aromatics and polar compounds (3, 4, and 5+ polars rings) than DAO 2 and raffinate 1. The aromatic extract also exhibits an important decrease in the proportion of saturate compounds compared to DAO 2. In contrast, raffinate 1 has a similar composition to DAO 2, but with a higher content of saturate compounds.

Figure 2C presents the percentage of different fractions for the dewaxing unit, the samples raffinate 2 and BSS. In Figure 2C, both samples have the same pattern. As expected, a decrease in Sat compounds can be observed due to the dewaxing process. Mono- and diaromatic compounds, which are known for their lubrication properties, increase in BSS.

As viscosity is an important specification for lubricants, all the units were tuned to obtain the targeted viscosity value. Thus, it is particularly interesting to correlate viscosity to other chemical parameters to improve the understanding of the processes taking place in the different production units. As proposed by Mehrkesh et al. [2], the log of viscosity has been compared with the % of polyaromatics, calculated here as the sum of 2 rings, 3 rings, 4 rings, 5+ rings and polar compounds obtained by HPLC3. Table 2 presents the obtained percentage of aromatics for each sample.

Table 2. Percentage of monoaromatics and multiple aromatics in each sample.

Samples	Saturates (%w)	Percentage Mono Aromatic (%w)	Percentage Multiple Aromatics 2R-5R (%w)
VR	16.3	12.3	66.7
DAO 1	36.5	19.1	32.1
DAO 2	37.5	20.4	30.4
Raffinate 2	53.9	15.7	12.2
Aromatic Extract	11.9	26.2	63.6
Raffinate 3	52.3	12.1	15.7
BSS	48.0	19.1	17.1

Figure 3A presents the percentage of monoaromatics as a function of the logarithm of the viscosity for the seven samples, except for the VR. VR is the only sample of the series that contains asphaltene. It can be supposed that, due to its aggregation tendency [28], asphaltene has a large impact on viscosity. Thus, this sample has not been considered for the correlation. Figure 3B presents the correlation with the sum of all the polyaromatics (2/3/4/5 cores). The percentage of monoaromatics was less correlated with the log of viscosity with an $r^2 = 0.75$. In contrast, Figure 3B shows a linear trend between the aromatic content and viscosity, with $r^2 = 0.96$.

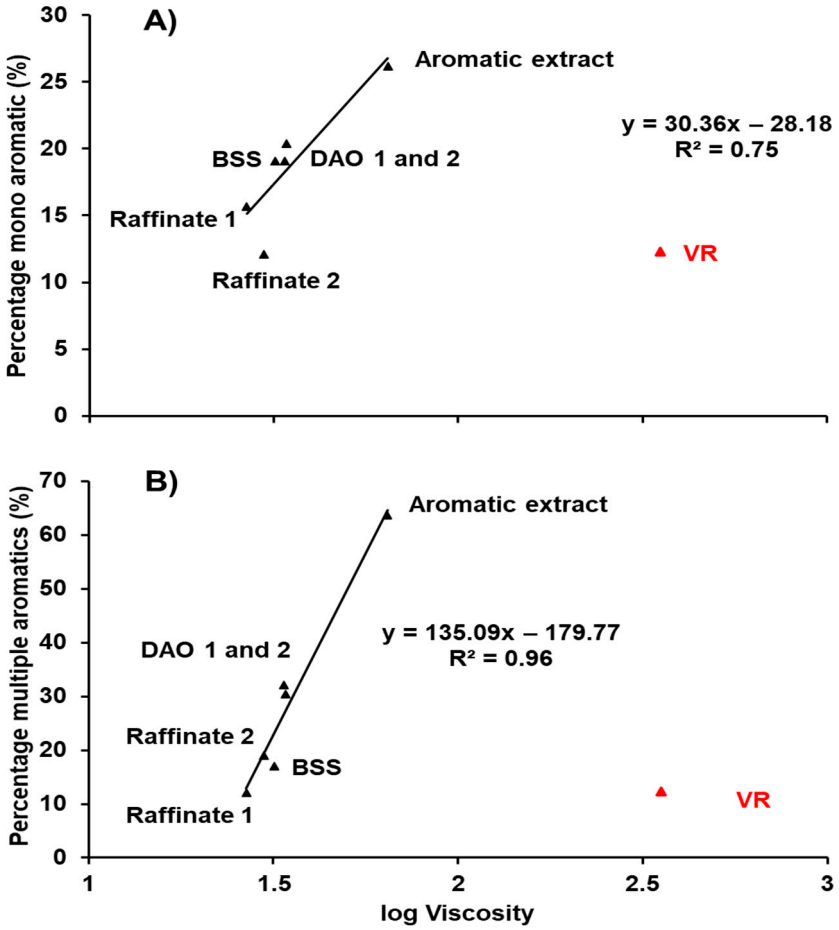

Figure 3. Correlation between the percentage of monoaromatic (**A**) and multiple aromatic (**B**) compounds and the log of viscosity for all the samples except vacuum residue (VR) (in red) and wax.

3.2. GPC-ICP HR MS Results

GPC is a chromatographic technique used to separate molecules or aggregates according to their hydrodynamic volume. Coupling GPC with an elemental detector such as ICP HR MS helps to determine the speciation of the different elements contained in petroleum samples, such as sulfur and metals. In previous works, the aggregation state of ^{32}S- and ^{51}V-containing molecule/aggregates [9,31,36] in different types of samples was studied. In particular, in the study by Desprez et al. [9], GPC-ICP HR MS was used to demonstrate a correlation between viscosity and specific, highly aggregated sulfur compounds in crude Oil, AR, VGO, and VR samples. To further understand the chemical parameters that impact viscosity, all the samples were analyzed by GPC-ICP HR MS to measure ^{32}S- and ^{51}V-containing molecules/aggregates. The results obtained for ^{32}S by GPC-ICP HR MS for all eight samples are presented in Figure 4 and Table 3.

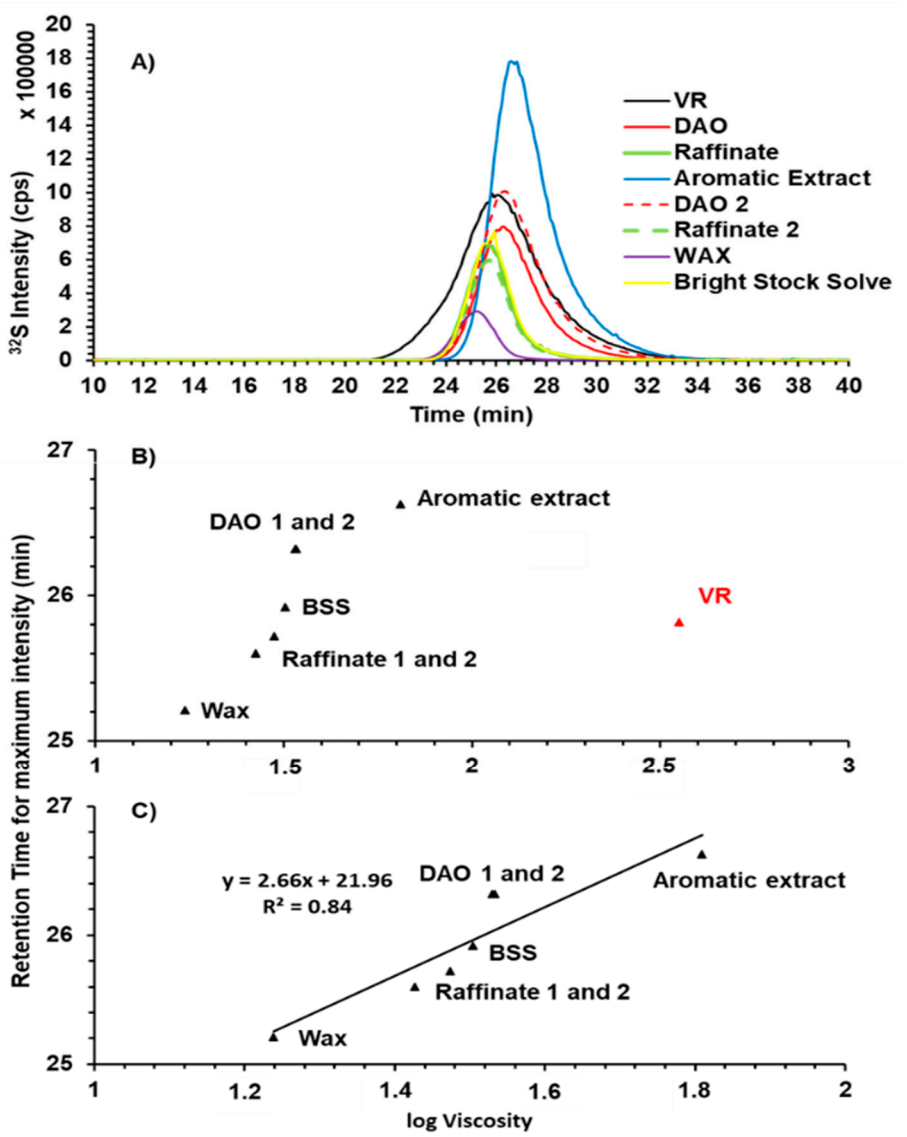

Figure 4. Chromatogram of sulfur containing molecules by GPC with inductively coupled plasma mass spectrometry (GPC-ICP HR MS) for all the samples (**A**). Retention time at the maximum intensity as a function of the log of viscosity for all the samples (**B**) and without VR (**C**). Abbreviations: GPC: gel permeation chromatography; ICP: inductively coupled plasma; MS: mass spectrometry

Table 3. Retention time at maximum intensity and at 10% maximum intensity for ^{32}S obtained by GPC-ICP HR MS for each sample.

Sample Name	Area for ^{32}S	Retention Time at Intensity Max (min)	x_1 at 10% Intensity Max (min)	x_2 at 10% Intensity Max (min)	Ratio x_2/x_1
VR	4114574	25.82	22.49	30.57	1.42
DAO 1	2302789	26.33	24.31	29.66	1.65
DAO 2	3094691	26.33	24.31	30.06	1.85
Raffinate 2	1477765	25.62	24.01	27.84	1.37
Aromatic Extract	5092305	26.63	24.92	30.46	2.24
Raffinate 3	1263077	25.72	24.01	27.84	1.24
BSS	1534473	25.92	24.11	27.84	1.06
Wax	550407	25.22	23.60	26.83	1.00

Table 3 presents the retention time at maximum intensity for all samples. Figure 4A presents the intensity of ^{32}S for the eight samples as a function of the retention time of the aggregates containing sulfur in GPC. All the samples were eluted between 22 min (higher molecular weight) and 32 min

(lower molecular weight). The chromatogram is separated into three different fractions: high molecular weight (20/24 min), medium molecular weight (24/28 min) and low molecular weight (28/32 min) [31]. Figure 4B presents the retention time for the maximum intensity as a function of the log of viscosity. In Figure 4C, as for the HPLC3 results, VR was removed because it contains many asphaltenes not present in the other samples, which are refining products. Figure 4C shows the relationship between retention time and viscosity. According to the HPLC3 results, this relationship is correlated with the percentage of aromatics in the sample.

As can be observed in Figure 4, none of the peaks in the chromatogram are Gaussian; they present one main peak and a tail (a fraction of the lower molecular weight) eluted after the main peak. Desprez et al. [9] correlated the log of viscosity with the percentage of trapped compounds (compounds eluted after the main peaks, as can be seen in Figure 3), but only for crude oil samples. In the work of Desprez, the chromatogram was composed of two visible peaks. Here, it can only be observed that the peaks are not Gaussian towards the lower molecular weights. Here, x_1 and x_2 were used to study these trapped compounds (the asymmetry aspect of the curve). In Table 3, x_1 and x_2 represent the two retention times at 10% of the maximum intensity compared with the retention time at the maximum intensity. The higher the ratio x_2/x_1, the higher the quantity of compounds eluted after the main peak. Figure 5 presents the percentage of x_2 compared to x_1 as a function of the log of viscosity for the 7 samples after removal of the VR sample.

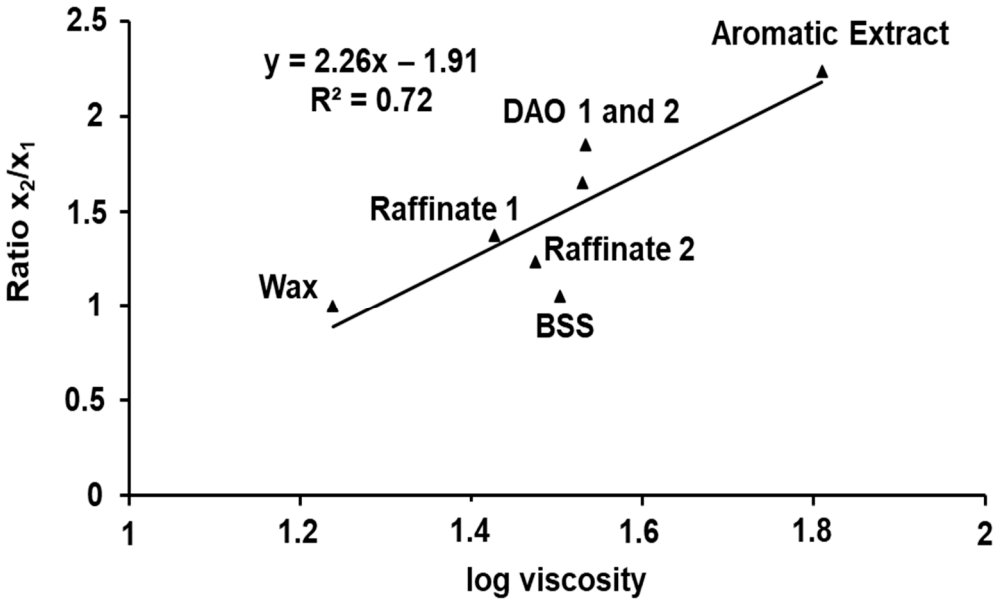

Figure 5. Ratio of x_2/x_1 as a function of the log of viscosity.

As can be seen in Figure 5, there is a relationship between the quantity of tailing after the main peak and the log of viscosity. These results, coupled with the amount of polyaromatics given by HPLC3, suggest that the aromatic compounds have a later elution time, as was already suggested by Panda et al. [10] and by Alawani et al. [5]. This result means that retention time, asymmetry of the curve, the percentage of aromatics, and viscosity are linked.

During this study, the signal of vanadium was also measured. Figure 6 presents the different chromatograms obtained.

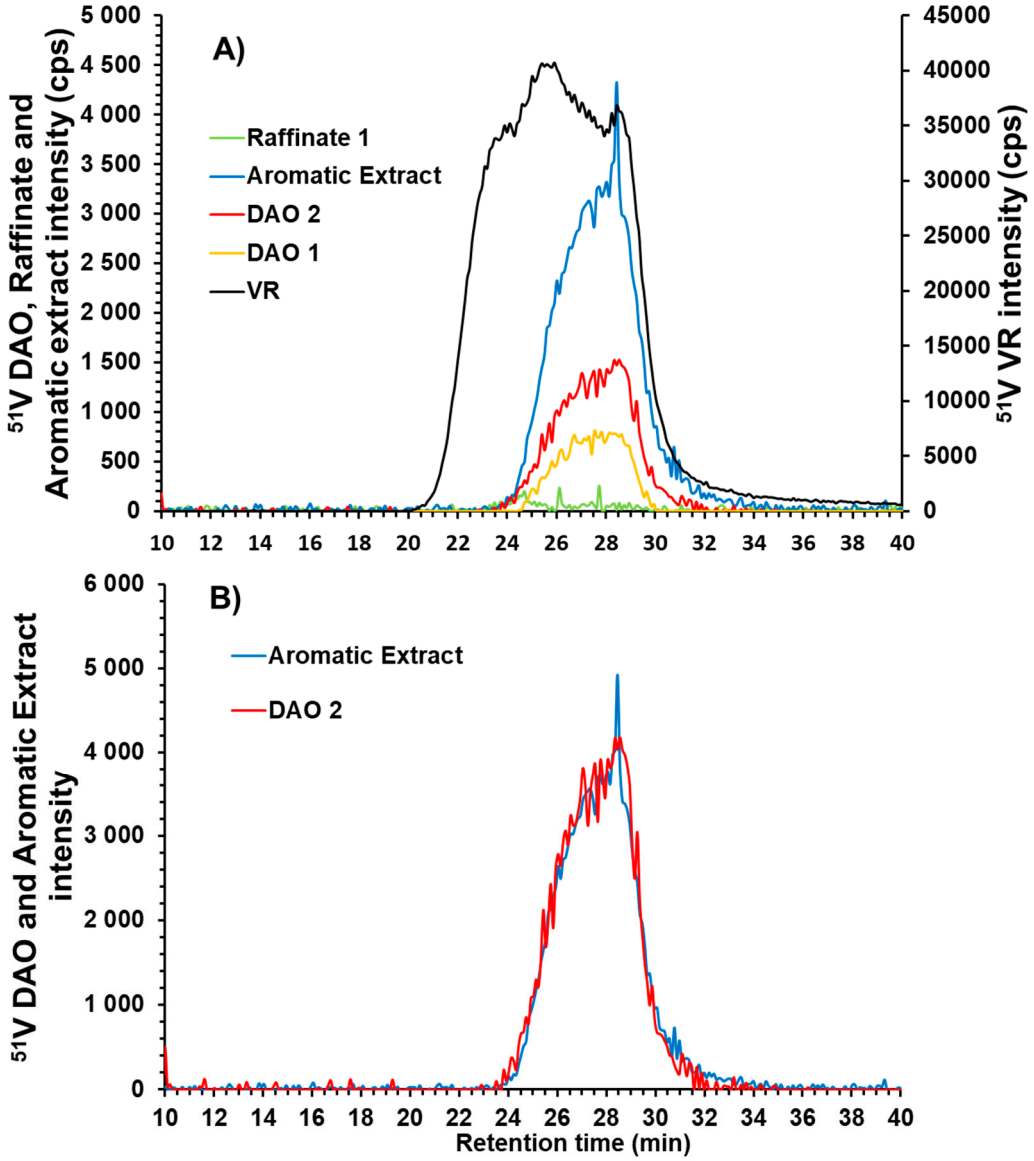

Figure 6. Chromatogram of vanadium-containing molecules by GPC-ICP HR MS for aromatic extract, de-asphalted oil (DAO 1), DAO feed of furfural (DAO 2), raffinate 1, and VR (**A**) and normalized chromatograms for aromatic extract and DAO 2 (**B**).

Figure 6A presents the intensity of ^{51}V as a function of the retention time in the GPC for VR, DAO 2, raffinate 1 and aromatic extract. The profile of vanadium-containing aggregates is trimodal for VR, as already observed for this kind of petroleum product [11,31]. As expected, HMW compounds containing ^{51}V were present in the VR sample (black line). Considered to be soluble nanoaggregates, these compounds were eliminated by the SDA unit. In contrast, a part of the low and medium molecular weights for ^{51}V remain in the DAO sample. The intensity of vanadium for DAO 1 and 2 are different. According to Table 1, the concentration of vanadium for these two samples was 1.6 and 2.2 ppm, respectively, which could be due to the tank effect, as the two samples come from different tanks - after the SDA unit (DAO 1) and before the FF unit (DAO 2). It is worth noting that all the remaining ^{51}V from the DAO was concentrated in the aromatic extract sample. This result is consistent with the high aromaticity of the supposed porphyrinic structure of ^{51}V-containing molecules. it should also be noted that furfural, used to produce the aromatic extract in the FF unit, is also used to extract porphyrins in residual oil [37]. In Figure 6B, it can been seen the profile of ^{51}V for DAO (red line)

and aromatic extract (blue line) normalized to the same area. Note that both profiles are identical, indicating that the FF unit induces no chemical change for vanadium-containing molecules.

3.3. APPI/APCI FT ICR Results

To determine the molecular composition of these samples, they were analyzed by FT-ICR MS. The APPI source promotes the ionization of the protonated molecules $[M + H]^+$ and/or cation radicals $M^{+\bullet}$ [16,17]. Paraffinic species, on the other hand, are not detectable in APPI+ but could be ionized in positive mode APCI using small alkanes, such as heptane as the solvent, yielding [M − H]+ ions through a hydride abstraction reaction [14]. These paraffinic species were mainly found in the wax and raffinate samples.

In the recorded APPI mass spectra, mostly $M^{+\bullet}$ radical cations were observed. Thus, in the following discussion, only these radical cations are considered. Figure 7 shows the DBE vs. C# plot for the HC and S_1 chemical classes of the radical species detected by APPI+ in the VR and DAO 1 samples.

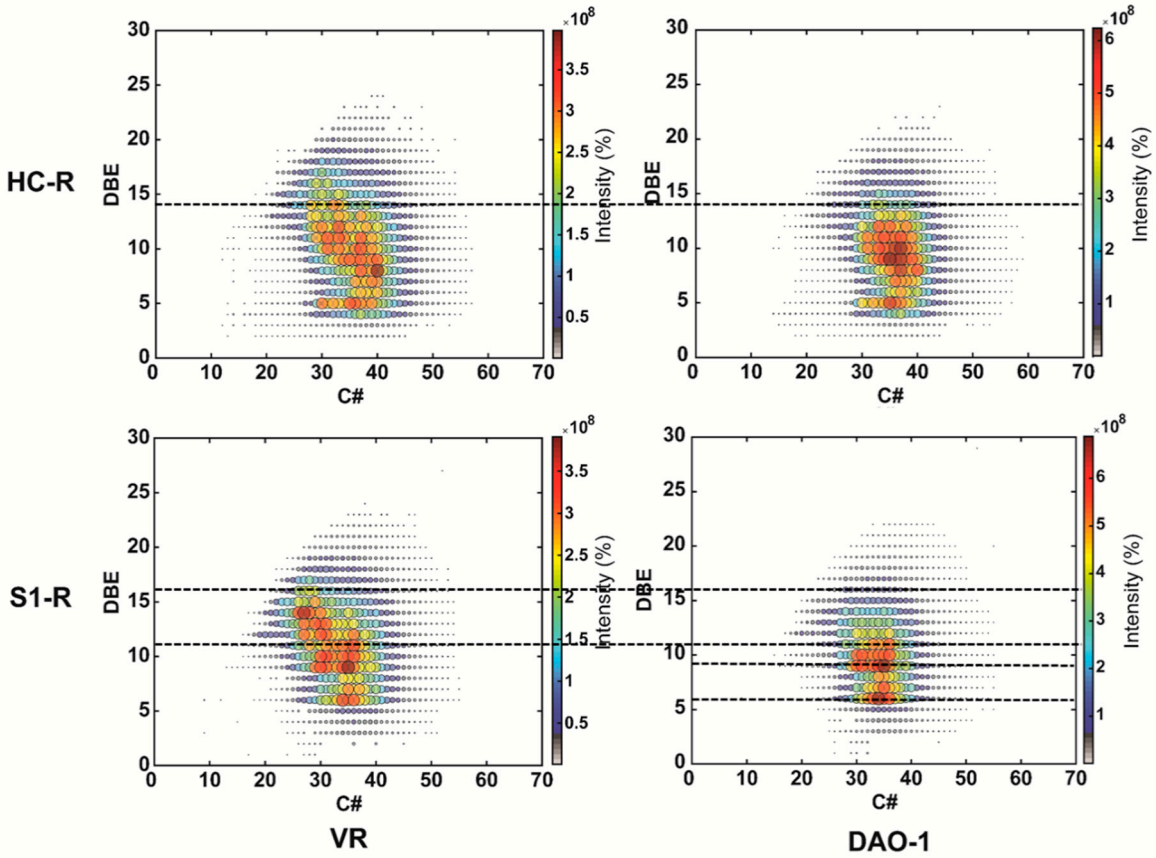

Figure 7. Double bond equivalent (DBE)/C# maps of the HC and S_1 chemical classes showing the cation radical species detected by the atmospheric pressure photo ionization (APPI) ± Fourier transformation ion cyclotron resonance (FT-ICR) mass spectra of VR (feed) and deasphalted oil (DAO) obtained from the SDA unit.

It can be observed that for both the S_1 and HC classes, the DAO 1 compound loses more aromatic (high DBE) compounds than the VR feed. In the HC class, a strong decrease of molecules with DBE higher than 14 is found. In the same way for the S_1 class, a strong decrease of molecules with DBE higher than 11 is found. This situation is consistent with the propane deasphalting process, which is expected to precipitate asphaltenes that contain the most aromatic species. Note that for sulfur-containing compounds, most species are between DBE 9 and 16 in the VR sample and between DBE 9 and 11 in the DAO 1 sample. Two series emerge for the S_1 class the in DAO 1 sample, at DBE 6 and 9. These series most certainly represent alkyl-benzothiophene (BT) and alkyl-dibenzothiophene (DBT) molecules,

respectively, which correspond to the one- and two-ring class species in HPLC3. For the HC class, two ion series are detected. The first series corresponds to the DBE 5 species, most likely naphthenic molecules. The other series, centered at DBE 10, involves mainly aromatic species.

Figure 8 shows the DBE vs. C# plot of the HC and S_1 chemical classes of the radical species detected by APPI+ in the DAO 2, raffinate 1, and aromatic extract samples.

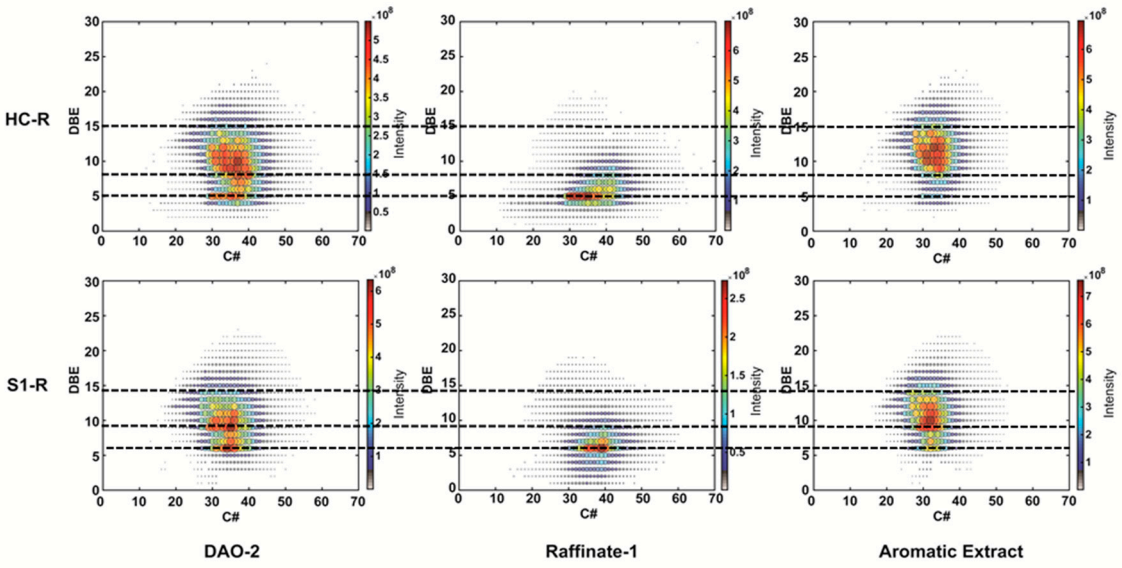

Figure 8. DBE/C# maps of the HC and S_1 chemical classes of the radical species detected by APPI+ in DAO 2, raffinate 1, and aromatic extract for the FF unit.

In Figure 8, the comparison of the three samples shows that the molecules have been selectively fractionated in the raffinate and aromatic extract using the furfural extraction process. In particular, for the S_1 family, it can be seen that the alkyl-BT species (DBE 6) are in raffinate, whereas the alkyl-DBT species are in the aromatic extract [28]. Furthermore, for the HC class, the naphthenic compounds (DBE 5) are in raffinate, whereas the more aromatic species are in the aromatic extract. This finding is consistent with the result of the HPLC3 analysis, which showed that most of the aliphatic species were mainly present in raffinate 1 as paraffinic (linear and/or branched) and naphthenic compounds. As the APPI source does not allow the detection of paraffins, they do not appear on the molecular maps shown in Figure 8. As expected, most of the aromatic species in the aromatic extract sample are found between DBE 8 and 15 for the HC family and between 9 and 14 for the S_1 class.

For the Dewaxing unit, as paraffins are not detectable in APPI+, the raffinate 2, BSS, and wax samples were analyzed using APCI+ [38], which allows the ionization of alkanes through the hydride abstraction processes with heptane as the solvent [21,39]. Figure 9 shows the DBE vs. C# plot of the HC and S_1 chemical classes according to the $[M - H]^+$ and/or $[M + H]^+$ electron ions in the samples.

The comparison of the raffinate fractions in Figures 8 and 9 highlights the use of APCI to effectively ionize the saturated compounds. In Figure 9, for HC and S_1, the aromatic compounds present in raffinate 2 are found in BSS, and paraffin is found in wax. As in the HPLC3 and GPC-ICP HR MS results, raffinate 2 and BSS are similar. For BSS, the same important series as are found in raffinate 2 are found in DBE from 4–7 for the HC family and in DBE 5–6 for the S_1 family. A significant decrease in paraffinic compounds at DBE 0 is observed in BSS.

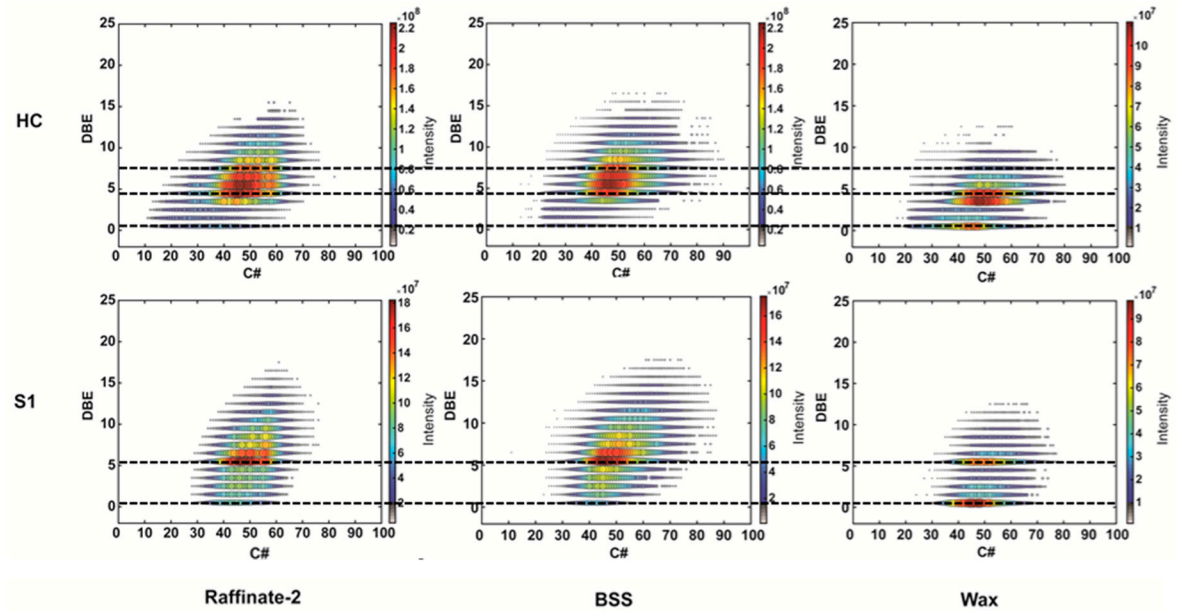

Figure 9. DBE/C# maps of the HC and S_1 chemical classes of proton species detected in atmospheric pressure chemical ionization (APCI)+ in raffinate 1, solvent extracted bright stock (BSS), and wax for the DEWAXING unit.

These paraffinic species are extracted in wax; in wax samples the maps show a series with high intensity at DBE 0 for HC and S_1, representing alkanes of the *n*-paraffin or isoparaffinic type. The main families in the HC series at DBE 3 and 4 represent cycloparaffins, polynaphthenic or monoaromatic species. For the S_1 family, the series with DBE 0 is also very much in the majority, representing structures of the thiol and/or thioether type. A second series at DBE 5 is clearly represented in the wax samples. As shown in Figure 9, compounds in the S_1 family of DBE 6, including benzothiophene sulfur compounds, are disappearing. However, this DBE 5 series is either residual aromatic compounds or naphthenic compounds. These may be cyclopentathiophene-type structures or thioethers/thiols with naphthenic rings. Looking at the intensity ratios, there is a 50% decrease in the intensity of the DBE 5 series for wax compared to the intensities in raffinate and BSS, showing that a small amount of DBE 5 sulfur compounds are present in wax.

In regards to the HPLC3 and GPC-ICP HR MS results, correlations between the FT-ICR MS results and the log of viscosity were made (Figure 10). Table 4 shows all the results that could be extracted from the S1 and HC plot. nC min represents the minimum carbon number, where peaks were found for each sample for the plot of HC and S_1. In the same way, nC max represents the maximum carbon number. DBE min and max represent the same for DBE. The HC and DBE size map represents the difference between the minimum and the maximum. A high DBE, or at least a high ratio of nC/DBE, suggests the presence of aromatics compounds. The HPLC3 and GPC-ICP-MS results suggest that aromatics compounds were correlated with the log of viscosity.

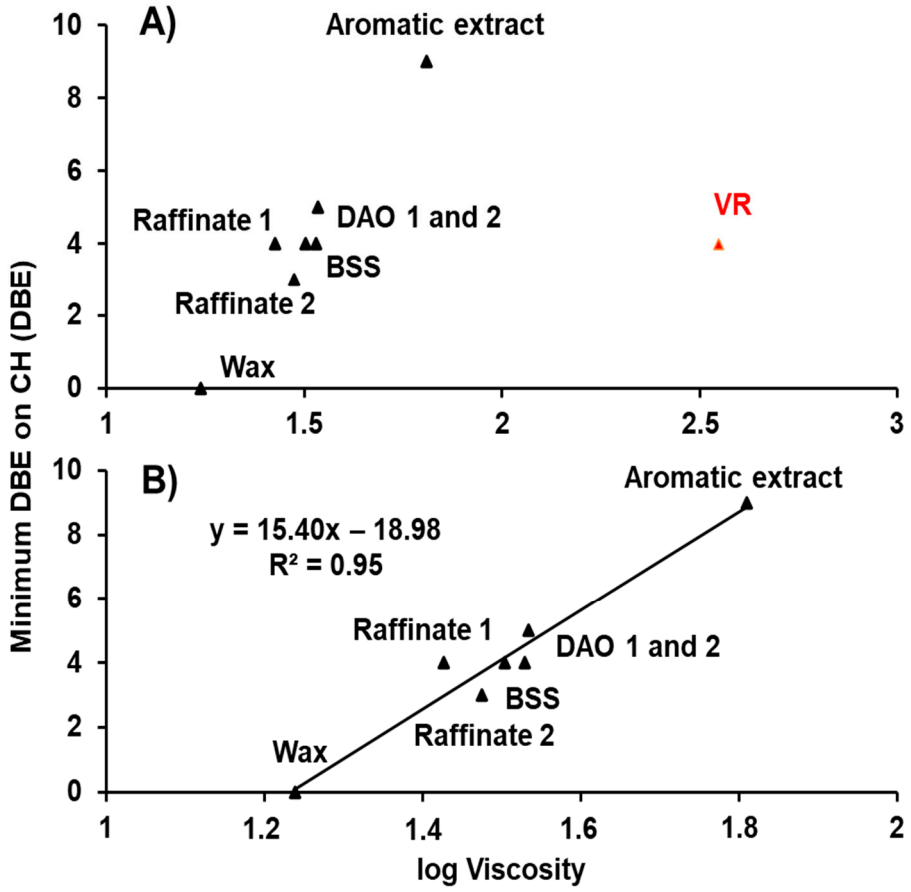

Figure 10. Minimum of DBE as a function of the log of viscosity for all the samples (**A**) except VR (**B**).

Table 4. Carbon number and DBE min and max data extracted from HC and S_1 (Figures 7–9).

		CH						S_1					
		nC min	nC max	nC Size Map	DBE min	DBE max	DBE Size Map	C min	C max	nC Size Map	DBE min	DBE max	DBE Size Map
SDA	VR	29	41	12	4	14	10	26	39	13	6	16	10
	DAO 1	29	39	10	4	14	10	28	39	11	6	13	7
FF	DAO 2	29	39	10	5	14	9	28	39	11	6	14	8
	Raffinate 1	30	43	13	4	8	4	30	43	13	6	9	3
	Aromatic Extract	28	39	11	9	15	6	26	38	12	6	14	8
Dewaxing	Raffinate 2	40	60	20	3	8	5	40	58	18	0	9	9
	BSS	38	58	20	4	8	4	38	60	22	0	9	9
	Wax	40	60	20	0	6	6	40	56	16	0	5	5

Figure 10 shows the minimum of DBE found in the HC maps for all the samples (Figure 10A), except VR (Figure 10B), as a function of the log of viscosity. As expected, VR was not correlated with the other samples. A linear correlation was found between the minimum DBE and the log of viscosity for all the other samples. Other correlations with nC max and min, as well as DBE max, did not show good correlation and are not shown here.

3.4. Statistic Treatment Using PLS Regression

By using three different advanced analytical techniques, it appears that, as suggested by several works [2,6,9], several parameters influence the viscosity of the sample. The HPLC3 data confirmed that the log of viscosity was correlated with the percentage of aromatics. The GPC-ICP HR MS data confirmed that the log of viscosity was correlated with the retention time of the maximum ^{32}S intensity.

Finally, the FT-ICR MS results suggested that the log of viscosity was correlated with the minimum of DBE for the HC map.

Statistical techniques were used to determine which variables affected viscosity. For this determination, all of the variables given by the three techniques (Tables 2–4), plus the variables given in Table 1, were correlated with the logarithm of viscosity. As before, VR was removed for the statistical treatment because this sample did not correlate with viscosity, probably due to its non-negligible asphaltene content. The results are given in Figure 11.

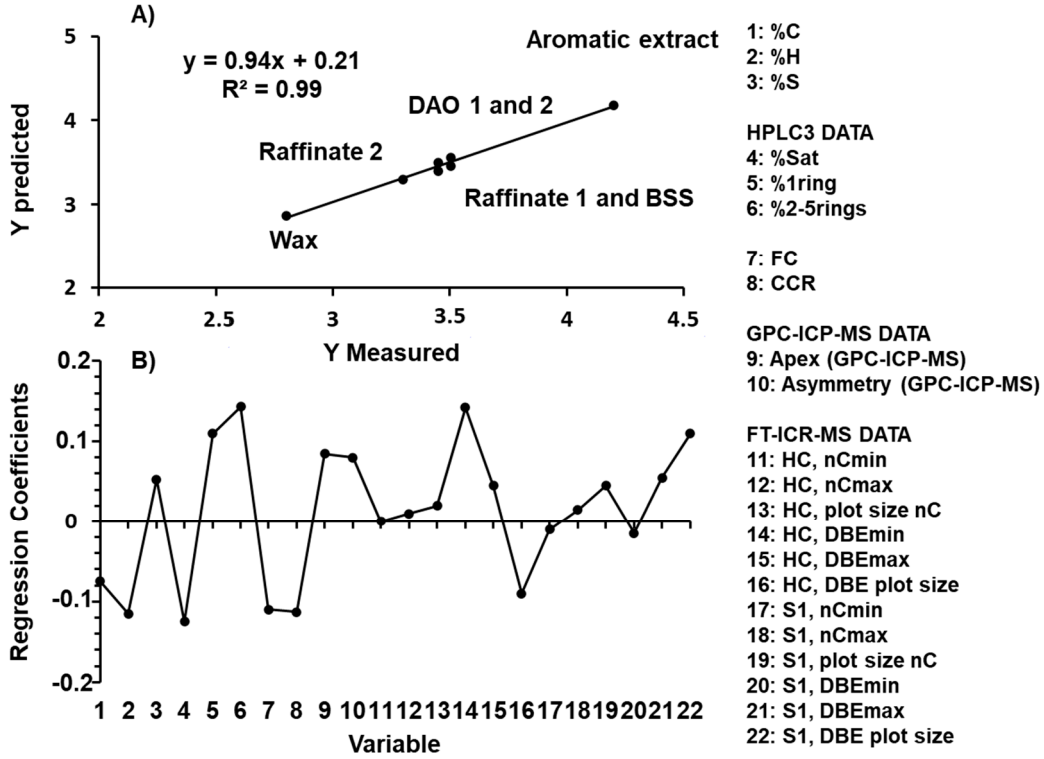

Figure 11. Calibration curves between the viscosity predicted by partial least square (PLS) and measured (**A**) except for the VR sample. Influence of 22 different variables on viscosity (**B**).

It can be seen in Figure 11A that the use of all these parameters provides a good correlation (R^2 = 0.97) between the log of the measured viscosity (Y measured) and the viscosity predicted by PLS (Y predicted). Figure 11B shows which parameters have a large influence on viscosity. It appears that viscosity increases when the percentage of sulfur, the percentage of one ring and polyaromatics (2R−5R), the retention time at maximum intensity, and the asymmetry ratio x_2/x_1 increases. These results confirm those presented in Figures 4 and 5, which showed that viscosity increased with the maximum intensity of the ^{32}S peak and asymmetry. The PLS results also suggest that the more sulfur there is in the samples, the more the viscosity increases, which could be explained by the possibility that sulfur is mainly present in aromatic compounds, such as BT and DBT, as suggested by the FT-ICR MS results in Figures 7–9, as well as the HPLC3 results in Figure 2. In contrast, the logarithm of viscosity decreased when the quantity of hydrogen, the percentage of Sat, the FC, and the CCR increased. FC represents the quantity of paraffin. Paraffin did not contain aromatic compounds and, as has already been stated, the log of viscosity increased with the quantity of aromatics. For hydrogen, meanwhile, a greater quantity of hydrogen suggested the presence of fewer aromatics compounds (and lower DBE), which is in agreement with the FT-ICR MS results.

To help daily optimization of the unit, it is necessary to develop a model using accessible data, such as elemental content. The advanced analytical techniques used in this article confirmed that viscosity is mainly linked to the aromatic and sulfur contents. Considering these results, it has been

tried to construct another PLS model with data available daily in a refinery. The aromatic content is linked to the C and H contents, while the S content is linked to CCR. The results are presented in supplemental information (Figure S1). It should be noted that the trends for the new model are the same as in the previous, more complex model. Viscosity increased when the % H decreased and when the % C and the % S increased.

Obviously, a model with seven points is not directly useful in a refinery. It should be noted that only one feedstock was used for this study, and the conclusions cannot be applied to all the samples used in a refinery. However, these results can predict tendencies and assist with the daily optimization of the unit. The development of a refining model would certainly require the use of molecular data, such as those acquired during this study. Such a model would allow us to describe more accurately the differences between two different feedstocks.

4. Conclusions

The aim of this study was to better understand the refining process of lubricants from a molecular point of view. The analytical techniques used in this study allowed us to identify and characterize the hydrocarbon-, sulfur-, and vanadium-containing compounds present in the different samples. The combination of three advanced analytical techniques (HPLC3, GPC-ICP HR MS and FT-ICR MS), all usually measurable in refinery data on lubricating oil base samples and statistic treatment, allowed the viscosity of a lubricating oil base sample to be predicted. Viscosity increases when the percentage of sulfur, the percentage of mono- and polyaromatics (2R−5R), the apex, and the asymmetry increase. In contrast, the logarithm of the viscosity decreases when the hydrogen content, the percentage of Sat, and the FC increase. This study showed the importance and effectiveness of cross-checking results with different complementary analytical techniques to acquire valuable data on lubricating oil base samples. This kind of methodology can be used for other types of samples or matrices. Furthermore, the relation between viscosity and different parameters of the lubricants can help for the daily optimization of the refinery unit.

Supplementary Materials: The following are available online at http://www.mdpi.com/2227-9717/8/11/1472/s1, Figure S1: Calibration curves between viscosity predicted by the second PLS model and measured (**A**) except for the VR sample. Influence of four different variables on the viscosity (**B**).

Author Contributions: Conceptualization and resources, C.B.-M. and P.G.; methodology, R.M., R.R., B.B., C.A., P.G. and C.B.-M.; formal analysis and data curation R.M. and J.L.M.; supervision, R.R., B.B., C.A., P.G. and C.B.-M.; writing—original draft preparation, R.M., J.L.M. and C.B.-M.; writing—review and editing, R.M., H.L., R.R., B.B., C.A., P.G. and C.B.-M. All authors have read and agreed to the published version of the manuscript.

Funding: The authors thank TOTAL for supplying the oil samples and Jonathan Putman for HPLC3 experiments. Work was performed at the National High Magnetic Field Laboratory ICR User Facility, which is supported by the National Science Foundation Division of Chemistry through Cooperative Agreements DMR-1157490 and DMR-1644779 and the state of Florida. This work was also supported by Conseil Régional d'Aquitaine (20071303002PFM) and FEDER (31486/08011464). The authors thank the EU for funding via the ERC PRIMCHEMproject (No. 636829). This work was supported at the Chimie Organique Bioorganique Réactivité Analyse (COBRA) laboratory by the European Regional Development Fund (ERDF) No. HN0001343, the European Union's Horizon 2020 Research Infrastructures program (grant agreement 731077), the national FT-ICR network (FR 3624 CNRS), the Région Normandie, and the Laboratoire LabEx SynOrg (ANR-11-LABX-0029).

Conflicts of Interest: The authors declare no conflict of interest.

References

1. Wilson, R.E.; Keith, P.C.; Haylett, R.E. LIQUID PROPANE Use in Dewaxing, Deasphalting, and Refining Heavy Oils. *Ind. Eng. Chem.* **1936**, *28*, 1065–1078. [CrossRef]
2. Mehrkesh, A.H.; Hajimirzaee, S.; Hatamipour, M.S. A Generalized Correlation for Characterization of Lubricating Base-oils from Their Viscosities. *Chin. J. Chem. Eng.* **2010**, *18*, 642–647. [CrossRef]
3. Kemp, L.C., Jr.; Hamilton, G.B.; Gross, H.H. Furfural as a Selective Solvent in Petroleum Refining. *Ind. Eng. Chem.* **1948**, *40*, 220–227. [CrossRef]

4. Varotsis, N.; Pasadakis, N. Rapid Quantitative Determination of Aromatic Groups in Lubricant Oils Using Gel Permeation Chromatography. *Ind. Eng. Chem. Res.* **1997**, *36*, 5516–5519. [CrossRef]
5. Alawani, N.A.; Panda, S.K.; Lajami, A.R.; Al-Qunaysi, T.A.; Muller, H. Characterization of Crude Oils through Alkyl Chain-Based Separation by Gel Permeation Chromatography and Mass Spectrometry. *Energy Fuels* **2020**, *34*, 5414–5425. [CrossRef]
6. Wang, F.C.-Y.; Zhang, L. Chemical Composition of Group II Lubricant Oil Studied by High-Resolution Gas Chromatography and Comprehensive Two-Dimensional Gas Chromatography. *Energy Fuels* **2007**, *21*, 3477–3483. [CrossRef]
7. Manheim, J.; Wehde, K.; Zhang, W.T.J.; Vozka, P.; Romanczyk, M.; Kilaz, G.; Kenttämaa, H.I. Identification and Quantitation of Linear Alkanes in Lubricant Base Oils by Using GC × GC/EI TOF Mass Spectrometry. *J. Am. Soc. Mass Spectrom.* **2019**, *30*, 2670–2677. [CrossRef]
8. Liang, Z.; Chen, L.; Alam, M.S.; Rezaei, S.Z.; Stark, C.; Xu, H.; Harrison, R.M. Comprehensive chemical characterization of lubricating oils used in modern vehicular engines utilizing GC × GC-TOFMS. *Fuel* **2018**, *220*, 792–799. [CrossRef]
9. Desprez, A.; Bouyssiere, B.; Arnaudguilhem, C.; Krier, G.; Vernex-Loset, L.; Giusti, P. Study of the Size Distribution of Sulfur, Vanadium, and Nickel Compounds in Four Crude Oils and Their Distillation Cuts by Gel Permeation Chromatography Inductively Coupled Plasma High-Resolution Mass Spectrometry. *Energy Fuels* **2014**, *28*, 3730–3737. [CrossRef]
10. Panda, S.K.; Alawani, N.A.; Lajami, A.R.; Al-Qunaysi, T.A.; Muller, H. Characterization of aromatic hydrocarbons and sulfur heterocycles in Saudi Arabian heavy crude oil by gel permeation chromatography and ultrahigh resolution mass spectrometry. *Fuel* **2019**, *235*, 1420–1426. [CrossRef]
11. Putman, J.C.; Sama, S.G.; Barrère-Mangote, C.; Rodgers, R.P.; Lobinski, R.; Marshall, A.G.; Bouyssiere, B.; Giusti, P. Analysis of Petroleum Products by Gel Permeation Chromatography Coupled Online with Inductively Coupled Plasma Mass Spectrometry and Offline with Fourier Transform Ion Cyclotron Resonance Mass Spectrometry. *Energy Fuels* **2018**, *32*, 12198–12204. [CrossRef]
12. Duan, P.; Qian, K.; Habicht, S.C.; Pinkston, D.S.; Fu, M.; Kenttämaa, H.I. Analysis of Base Oil Fractions by $ClMn(H_2O)^+$ Chemical Ionization Combined with Laser-Induced Acoustic Desorption/Fourier Transform Ion Cyclotron Resonance Mass Spectrometry. *Anal. Chem.* **2008**, *80*, 1847–1853. [CrossRef] [PubMed]
13. Nyadong, L.; Quinn, J.P.; Hsu, C.S.; Hendrickson, C.L.; Rodgers, R.P.; Marshall, A.G. Atmospheric Pressure Laser-Induced Acoustic Desorption Chemical Ionization Mass Spectrometry for Analysis of Saturated Hydrocarbons. *Anal. Chem.* **2012**, *84*, 7131–7137. [CrossRef]
14. Hourani, N.; Muller, H.; Adam, F.M.; Panda, S.K.; Witt, M.; Al-Hajji, A.A.; Sarathy, S.M. Structural Level Characterization of Base Oils Using Advanced Analytical Techniques. *Energy Fuels* **2015**, *29*, 2962–2970. [CrossRef]
15. Putman, J.C.; Rowland, S.M.; Podgorski, D.C.; Robbins, W.K.; Rodgers, R.P. Dual-Column Aromatic Ring Class Separation with Improved Universal Detection across Mobile-Phase Gradients via Eluate Dilution. *Energy Fuels* **2017**, *31*, 12064–12071. [CrossRef]
16. Bae, E.; Na, J.-G.; Chung, S.H.; Kim, H.S.; Kim, S. Identification of about 30,000 Chemical Components in Shale Oils by Electrospray Ionization (ESI) and Atmospheric Pressure Photoionization (APPI) Coupled with 15 T Fourier Transform Ion Cyclotron Resonance Mass Spectrometry (FT-ICR MS) and a Comparison to Conventional Oil. *Energy Fuels* **2010**, *24*, 2563–2569. [CrossRef]
17. Purcell, J.M.; Hendrickson, C.L.; Rodgers, R.P.; Marshall, A.G. Atmospheric Pressure Photoionization Fourier Transform Ion Cyclotron Resonance Mass Spectrometry for Complex Mixture Analysis. *Anal. Chem.* **2006**, *78*, 5906–5912. [CrossRef]
18. Jin, C.; Viidanoja, J.; Li, M.; Zhang, Y.; Ikonen, E.; Root, A.; Romanczyk, M.; Manheim, J.; Dziekonski, E.; Kenttämaa, H.I. Comparison of Atmospheric Pressure Chemical Ionization and Field Ionization Mass Spectrometry for the Analysis of Large Saturated Hydrocarbons. *Anal. Chem.* **2016**, *88*, 10592–10598. [CrossRef]
19. Tose, L.V.; Cardoso, F.M.; Fleming, F.P.; Vicente, M.A.; Silva, S.R.; Aquije, G.M.; Vaz, B.G.; Romão, W. Analyzes of hydrocarbons by atmosphere pressure chemical ionization FT-ICR mass spectrometry using isooctane as ionizing reagent. *Fuel* **2015**, *153*, 346–354. [CrossRef]

20. Mead, W.L. Field ionization mass spectrometry of heavy petroleum fractions. Waxes. *Anal. Chem.* **1968**, *40*, 743–747. [CrossRef]
21. Souza, L.M.; Tose, L.V.; Cardoso, F.M.R.; Fleming, F.P.; Pinto, F.E.; Kuster, R.M.; Filgueiras, P.R.; Vaz, B.G.; Romão, W. Evaluating the effect of ion source gas (N_2, He, and synthetic air) on the ionization of hydrocarbon, condensed aromatic standards, and paraffin fractions by APCI(+)FT-ICR MS. *Fuel* **2018**, *225*, 632–645. [CrossRef]
22. Manheim, J.; Zhang, Y.; Viidanoja, J.; Kenttämaa, H.I. An Automated Method for Chemical Composition Analysis of Lubricant Base Oils by Using Atmospheric Pressure Chemical Ionization Mass Spectrometry. *J. Am. Soc. Mass Spectrom.* **2019**, *30*, 2014–2021. [CrossRef] [PubMed]
23. Marshall, A.G.; Hendrickson, C.L.; Jackson, G.S. Fourier transform ion cyclotron resonance mass spectrometry. *Mass Spectrom. Rev.* **1998**, *17*, 1–35. [CrossRef]
24. Boldin, I.A.; Nikolaev, E.N. Fourier transform ion cyclotron resonance cell with dynamic harmonization of the electric field in the whole volume by shaping of the excitation and detection electrode assembly. *Rapid Commun. Mass Spectrom.* **2011**, *25*, 122–126. [CrossRef]
25. Chen, H.; Hou, A.; Corilo, Y.E.; Lin, Q.; Lu, J.; Mendelssohn, I.A.; Zhang, R.; Rodgers, R.P.; McKenna, A.M. 4 Years after the *Deepwater Horizon* Spill: Molecular Transformation of Macondo Well Oil in Louisiana Salt Marsh Sediments Revealed by FT-ICR Mass Spectrometry. *Environ. Sci. Technol.* **2016**, *50*, 9061–9069. [CrossRef]
26. Marshall, A.G.; Chen, T. 40 years of Fourier transform ion cyclotron resonance mass spectrometry. *Int. J. Mass Spectrom.* **2015**, *377*, 410–420. [CrossRef]
27. Hourani, N.; Andersson, J.T.; Möller, I.; Amad, M.; Witt, M.; Sarathy, S.M. Atmospheric pressure chemical ionization Fourier transform ion cyclotron resonance mass spectrometry for complex thiophenic mixture analysis. *Rapid Commun. Mass Spectrom.* **2013**, *27*, 2432–2438. [CrossRef]
28. Muller, H.; Adam, F.M.; Panda, S.K.; Al-Jawad, H.H.; Al-Hajji, A.A. Evaluation of Quantitative Sulfur Speciation in Gas Oils by Fourier Transform Ion Cyclotron Resonance Mass Spectrometry: Validation by Comprehensive Two-Dimensional Gas Chromatography. *J. Am. Soc. Mass Spectrom.* **2012**, *23*, 806–815. [CrossRef]
29. Loh, G.C.; Lee, H.-C.; Tee, X.Y.; Chow, P.S.; Zheng, J.W. Viscosity Prediction of Lubricants by a General Feed-Forward Neural Network. *J. Chem. Inf. Model.* **2020**, *60*, 1224–1234. [CrossRef]
30. Braga, J.W.B.; Junior, A.A.D.S.; Martins, I.S. Determination of viscosity index in lubricant oils by infrared spectroscopy and PLSR. *Fuel* **2014**, *120*, 171–178. [CrossRef]
31. Sama, S.G.; Desprez, A.; Krier, G.; Lienemann, C.-P.; Barbier, J.; Lobinski, R.; Barrere-Mangote, C.; Giusti, P.; Bouyssiere, B. Study of the Aggregation of Metal Complexes with Asphaltenes Using Gel Permeation Chromatography Inductively Coupled Plasma High-Resolution Mass Spectrometry. *Energy Fuels* **2016**, *30*, 6907–6912. [CrossRef]
32. Caumette, G.; Lienemann, C.-P.; Merdrignac, I.; Bouyssiere, B.; Lobinski, R. Element speciation analysis of petroleum and related materials. *J. Anal. At. Spectrom.* **2009**, *24*, 263–276. [CrossRef]
33. Giusti, P.; Ordóñez, Y.N.; Lienemann, C.-P.; Schaumlöffel, D.; Bouyssiere, B.; Łobiński, R. µFlow-injection–ICP collision cell MS determination of molybdenum, nickel and vanadium in petroleum samples using a modified total consumption micronebulizer. *J. Anal. At. Spectrom.* **2007**, *22*, 88–92. [CrossRef]
34. Zhang, L.; Hou, Z.; Horton, S.R.; Klein, M.T.; Shi, Q.; Zhao, S.; Xu, C. Molecular Representation of Petroleum Vacuum Resid. *Energy Fuels* **2014**, *28*, 1736–1749. [CrossRef]
35. Kim, S.; Kramer, R.W.; Hatcher, P.G. Graphical Method for Analysis of Ultrahigh-Resolution Broadband Mass Spectra of Natural Organic Matter, the Van Krevelen Diagram. *Anal. Chem.* **2003**, *75*, 5336–5344. [CrossRef] [PubMed]
36. Caumette, G.; Lienemann, C.-P.; Merdrignac, I.; Bouyssiere, B.; Lobinski, R. Fractionation and speciation of nickel and vanadium in crude oils by size exclusion chromatography-ICP MS and normal phase HPLC-ICP MS. *J. Anal. At. Spectrom.* **2010**, *25*, 1123–1129. [CrossRef]
37. Ali, M.F.; Abbas, S. A review of methods for the demetallization of residual fuel oils. *Fuel Process. Technol.* **2006**, *87*, 573–584. [CrossRef]

38. Řezanka, T.; Sigler, K. Identification of very long chain fatty acids from sugar cane wax by atmospheric pressure chemical ionization liquid chromatography–mass spectroscopy. *Phytochemistry* **2006**, *67*, 916–923. [CrossRef]
39. Aasen, A.J.; Hofstetter, H.H.; Iyengar, B.T.R.; Holman, R.T. Identification and analysis of wax esters by mass spectrometry. *Lipids* **1971**, *6*, 502–507. [CrossRef]